UNIVERSITY OF
BATH

University of Bath

Tuning the Mechanical Response of Metal-Organic Frameworks by Defect Engineering

Stefano Dissegna,[a] Pia Vervoorts,[a] Claire L. Hobday,[b] Tina Düren,[b] Dominik Daisenberger,[c] Andrew J. Smith,[c] Roland A. Fischer,[a*] Gregor Kieslich[a*]

[a] Chair of Inorganic and Metal-Organic Chemistry, Catalysis Research Center, Department of Chemistry, Technical University of Munich

Ernst-Otto-Fischer-Straße 1, 85748 Garching, Germany

[b] Centre for Advance Separations Engineering, Department of Chemical Engineering, University of Bath, Bath BA2 7AY, UK.

[c] Diamond Light Source, Diamond House, Harwell Science and Innovation Campus, Didcot, OX11 ODE Oxfordshire, UK.

Supporting Information Placeholder

ABSTRACT: The incorporation of defects into crystalline materials provides an important tool to fine-tune properties throughout various fields of materials science. We performed high-pressure powder X-ray diffraction experiments, varying pressures from ambient to 0.4 GPa in 0.025 GPa increments to probe the response of defective UiO-66 to hydrostatic pressure for the first time. We observe an onset of amorphization in defective UiO-66 samples around 0.2 GPa and decreasing bulk modulus as function of defects. Intriguingly, the observed bulk moduli of defective UiO-66(Zr) samples do not correlate with defect concentration, highlighting the complexity of how defects are spatially incorporated into the framework. Our results demonstrate the large impact of point defects on the structural stability of MOFs and pave the way for experiment-guided computational studies on defect engineered MOFs.

The ability to control structure-property relations in crystalline materials is at the heart of modern materials science.[1] In this pursuit, the targeted incorporation of defects is a crucial tool for fine-tuning properties throughout different areas of chemistry, such as condensed matter physics and materials science.[2-3] It is therefore exciting to see that defect engineering has recently entered the field of metal-organic frameworks (MOFs). MOFs are a relatively new class of framework materials, combining the versatility of organic chemistry with the library of inorganic metal nodes. The organic linker molecules bridge the inorganic building units to form 2D or 3D periodic networks often with guest-accessible porosity. The large chemical tunability in combination with the powerful concept of reticular chemistry in principle allows for designing MOFs to meet specific structural and chemical requirements.[4] In turn, MOFs offer great opportunities across many subjects of materials science ranging from catalysis,[5-7] sensors,[8] filters[9-10] to water harvesting systems[11-13] to name just a few. When considering the defect chemistry of MOFs in more detail, it was shown that macroscopic properties such as porosity and in turn catalytic activity and microscopic properties such as lattice dynamics are closely linked to the defect chemistry.[14-15,16] Furthermore, some MOFs can be transformed to amorphous and glassy states with the complete absence of long-range order.[17-18] In the context of point defects in crystalline MOFs, $M_6O_4(OH)_4(bdc)_6$ (UiO-66, M = Zr and Hf and H_2bdc = 1,4-benzendicarboxylic acid) and similiarly its dehydrated form $M_6O_6(bdc)_6$ are currently widely used in the community, owing to their high thermal and mechanical stability combined with a certain chemical robustness.[19] UiO-66 crystallizes in a face-centered cubic framework in **fcu** topology, with $[M_6O_6]^{12+}$ metal-nodes in 12-fold coordination of $(bdc)^{2-}$.[20] Synthetically, defects are typically incorporated by the so-called modulator approach, where high equivalents of monodentate acids such as formic acid, acetic acid and trifluoro acetic acid are added to the reaction mixture.[21-23] For small amounts of modulators, crystallinity of the defect-free framework is enhanced, whilst large amounts facilitate the incorporation of modulators into the structure and the formation of Schottky-type defects. Importantly, it was shown that under certain circumstances defect incorporation can occur in a correlated fashion, producing nanoregions with reduced **pcu** symmetry.[24]

The permanent porosity and low density implicate that MOFs are soft materials.[25] The large chemical diversity together with the potential to form highly connected lattices, however, lead to bulk moduli that span a range between K = 4 - 30 GPa.[26] In some cases, hydrostatic pressure can trigger porous-to-nonporous phase transitions in flexible model systems such as ZIF-4(Zn) and MIL-53(Al) at pressures as low as 0.05 GPa, making MOFs potential working media in mechanocalorics and mechanical dampers.[27-28] In the absence of structural and thermodynamic requirements for a porous-to-nonporous transition,[29] MOFs are prone to undergo amorphization at relatively low pressures.[25] For instance, MOF-5 amorphizes irreversibly by direct compression at pressures below 3.5 MPa and ZIF-8 at 0.34 GPa.[30-31] Such insight is not only fascinating from a fundamental viewpoint, but also tackles application-oriented questions, *e.g.* stability-issues of MOFs during shaping processes for catalytic applications.[32]
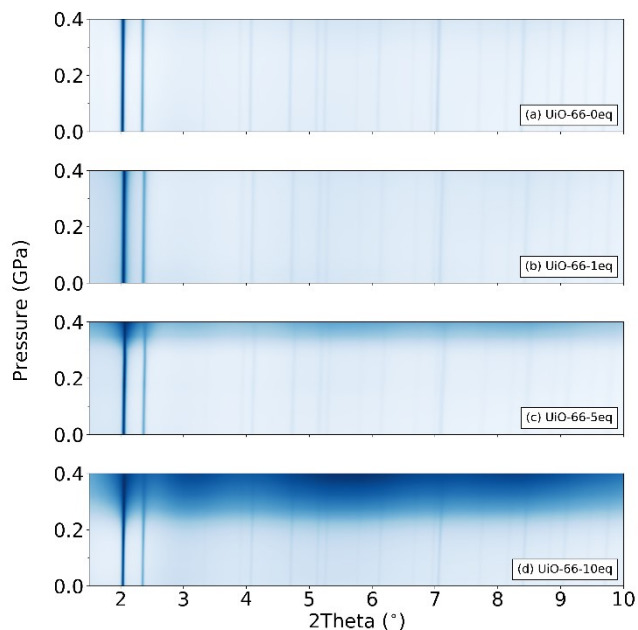
Figure 1. Contour plots of HPPXRD data (λ = 0.4246 Å) of UiO-66 without modulator (**a**), with 1 equivalent modulator (**b**), with 5 equivalents modulator (**c**) and 10 equivalents of modulator (**d**). High-pressure powder X-ray diffraction was measured in 0.025 GPa steps starting from 0.1 MPa, leading to 18 datasets between 0.1 MPa and 0.4 GPa. For better visualization the data was normalized before plotting and intensities between the respective pressure points are interpolated for clarity (blue = high relative intensities, white = low relative intensities).

Despite the on-going research interest in the defect chemistry of MOFs, experimental studies that address the mechanical stability of defective MOFs are presently absent in the literature. However, computational studies have been performed on UiO-66, its isoreticular expansions UiO-67 and UiO-68, HKUST-1, ZIF-8 and IRMOF-1.[33-38] Focusing on UiO-66,[33] van Speybroeck and co-workers performed an insightful computational study on defective UiO-66, addressing questions concerning the thermodynamics of defective UiO-66 under hydrostatic pressures. They find a small but significant impact of the spatial arrangements of defects on the onset pressure of amorphization and similarly the bulk modulus. Likewise, Thornton and co-workers highlighted the large parameter space of defective UiO-66, finding that highly defective UiO-66 with correlated defects (**reo** topology) exhibit a more stable structure compared to highly defective uncorrelated systems.[35] Following on from their important computational results, we herein apply high-pressure powder X-ray diffraction (HPPXRD) to characterize the mechanical response of defective MOFs to hydrostatic pressure experimentally with a non-penetrating transmitting media for the first time.

Defective UiO-66(Zr) samples were prepared by using trifluoro acetic acid (TFA) as modulator. In detail, three defective samples with 1 (**UiO-66-1eq**), 5 (**UiO-66-5eq**) and 10 (**UiO-66-10eq**) equivalents of TFA with respect to the zirconia concentration were prepared.[22] Unmodulated UiO-66 (**UiO-66-0eq**) was also synthesized as a reference sample, following a modified procedure reported by Shearer *et al.*[21] Laboratory powder X-ray diffraction was used to confirm phase purity for all samples (see SI figure S1). N$_2$ physisorption measurements and thermogravimetric analysis (TGA) show porosities and
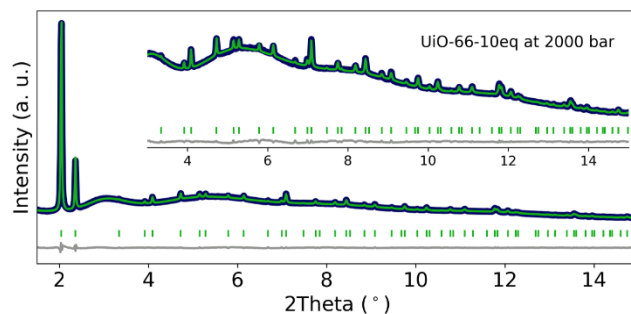

Figure 2. Representative HPPXRD pattern (λ = 0.4246 Å) of **UiO-66-10eq** (black) with and corresponding profile fits (colored curve) and difference curves (grey) at 0.2 GPa (Rwp = 1.81, χ^2= 0.42). The inset shows the diffraction data of the high angle region.

thermal stabilities that are in good agreement with the literature.[21] A quantification of the defect concentration (see SI figure S3 and table S1) was performed using TGA data, according to the method proposed by Valenzano *et al.*.[19] We find a defect concentration of approximately 3% for **UiO-66-0eq**, whilst TFA modulated samples **UiO-66-1eq**, **UiO-66-5eq** and **UiO-66-10eq** show a defect concentration of approximately 22.5%, 26.6% and 28.3%, respectively. Assuming only linker defects, the metal-nodes in defective materials exhibit a mean coordination number (CN) of 11.6 (**UiO-66-0eq**), 9.3 (**UiO-66-1eq**), 8.8 (**UiO-66-5eq**) and 8.6 (**UiO-66-10eq**) compared to 12 in the ideal, defect-free UiO-66 structure.

HPPXRD on soft materials with low pressures of amorphization is challenging, since a typical diamond anvil cell setup is designed for working pressures well above 0.1 GPa. Therefore, in this work we applied a radically different approach, using a HPPXRD setup which allows the application of pressure in small-increments in the range of p = ambient – 0.4 GPa (see SI for details).[39] In total, we collected 18 HPPXRD datasets for each sample with pressure increments of 0.025 GPa. Contour plots of the obtained HPPXRD pattern are shown in Figure 1, and stacking plots are given in the supporting information. Notably, we do not observe any intensities in the HPPXRD pattern related to a primitive superlattice that would indicate the formation of nano-regions of correlated defects. However, the absence of such superlattice reflections not excludes correlations on the sub-nano scale which are not

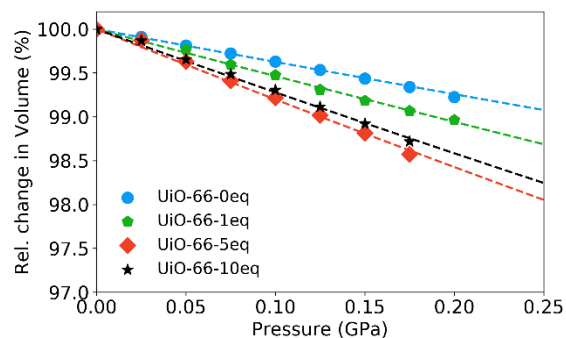**Figure 3**. Relative volumes as a function of pressure for **UiO-66-0eq** (blue), **UiO-66-1eq** (green), **UiO-66-5eq** (red) and **UiO-66-10eq** (black). The straight lines represent the fits of the 2nd order Birch-Murnaghan equation of states.

Table 1. Bulk moduli obtained in this work and comparison values for related 3D frameworks. Values marked with ¥ are from computational works.

Material	Bulk Modulus [GPa]	Reference
UiO-66-oeq	26.4 ± 0.13	This work
UiO-66-1eq	18.3 ± 0.16	This work
UiO-66-5eq	12.2 ± 0.18	This work
UiO-66-10eq	13.9 ± 0.22	This work
UiO-66	17	[41]
UiO-66¥	22¥	[33]
HKUST-1	30.7	[42]
ZIF-8	6.5	[31, 43]
[CH$_3$NH$_3$]PbI$_3$	14.9	[44]
[NH$_3$NH$_2$]Pb[HCOO]$_3$	19	[45]

detectable with X-ray diffractions techniques.[24] From the contour plots we already observe qualitatively that **UiO-66-oeq** and **UiO-66-1eq** remain crystalline up to a pressure of 0.4 GPa with no visual indication of peak broadening.[40] In contrast a clear loss of crystallinity appears around 0.3 GPa for **UiO-66-5eq** and at approximately 0.25 GPa for **UiO-66-10eq**. In order to quantify the onset pressure of amorphization quantitatively, we performed Pawley profile fits, see Figure 2 for an exemplary profile fit and SI for details. Analyzing the full width half maximum (FWHM) of the peaks as a function of pressure, no significant changes are observed for **UiO-66-oeq** and **UiO-66-1eq** until $p = 0.4$ GPa, see SI Figure S13. This confirms that hydrostatic conditions are maintained up to 0.4 GPa without evidence for loss of long-range order. For **UiO-66-5eq** and **UiO-66-10eq**, anomalies of the FWHM starting at pressures of $p = 0.275$ GPa and $p = 0.225$ GPa are observed. These anomalies are related to an onset of amorphization and agree with the trend found computationally.[33] The amorphization process is not reversible, hence is best described with a collapse of the framework under low hydrostatic pressures (see SI for PXRD pattern after compression).

We now turn our attention to the volume of the materials as function of pressure, $V(p)$, which we obtained from the profile fits. The bulk modulus which is defined as the inverse of the compressibility, *i.e.* $K = -V \cdot (dp/dV)$, is a measure for mechanic resistance of a material against volumetric changes under hydrostatic pressures. Since we observe unusual volume changes for pressures above approximately 0.2 GPa for the highly defective samples, see SI Figure S12, the bulk moduli were calculated by fitting a 2nd order Birch-Murnaghan equation of state[46] to the first 8 data points in our $V(p)$ data, *i.e.* up to pressures of $p = 0.175$ GPa (see Figure 3). We obtain values of K(**UiO-66-oeq**) = 26.4 ± 0.13 GPa, K(**UiO-66-1eq**) = 18.3 ± 0.16 GPa, K(**UiO-66-5eq**) = 12.2 ± 0.18 GPa and K(**UiO-66-10eq**) = 13.9 ± 0.22 GPa , see Figure 3 and Table 1. The origin of the discontinous behavior for pressures above 0.2 GPa for **UiO-66-5eq** and **UiO-66-10eq** itself is unclear. The discontionous change in the V(p) data is only observed for highly defective samples, in principle pointing to the occurrence of a phase transition; however, no other evidence were found in our diffraction data to back-up this conclusion and is subject of on-going studies. Comparing the bulk moduli of our reference sample **UiO-66-oeq** to literature data, we find UiO-66 being one of the least compliant MOFs, only beaten by

HKUST-1 with $K = 30$ GPa. The difference to previous meauserements, *e.g.* by Yot *et al*.[41] who report UiO-66 to exhibit a bulk modulus of $K = 17$ GPa highlights the impact of the preparation method on the mechanical response of the framework, *e.g.* activation and dehydration mechanisms and the potential presence of unintentional defect incorporation. For instance, the use of HCl in the synthesis of UiO-66 facilitates the decomposition of dimethylformamide into dimethylammonium and HCOO$^-$ at high temperatures which in turn can act as modulator in the synthesis. [21] The impact of the coordination of the metal node on the mechanical properties becomes evident when comparing the bulk modulus of **UiO-66-oeq** with dense coordination networks such as perovskite-type materials [CH$_3$NH$_3$]PbI$_3$ and [NH$_3$NH$_2$]Zn(HCOO)$_3$ that exhibit a 6-fold connectivity of the metal-node (Table 1).[45] Looking at the bulk moduli of the defective samples, the bulk modulus initially drops significantly. For instance, **UiO-66-1eq** exhibits a significant lower bulk modulus ($K = 18.3$ GPa), confirming computational results and the expectations that a defective framework is less stress resistant. Interestingly, **UiO-66-5eq** exhibits a slightly lower bulk modulus than the most defective sample **UiO-66-10eq**. This finding is counterintuitive at first sight, but reflects the complex structure-property relation when going from perfect UiO-66 in **fcu** topology (CN = 12) to hypothetical UiO-66 in **reo** topology (CN= 8). In between, different scenarios with different types and amounts of (correlated) defects are possible, depending on the kinetics and thermodynamics of formation. From our results it seems that with increasing amount of defects correlated regions become more likely, presumably leading to a higher bulk modulus while keeping the amorphization onset low. From zeolites it is known that the correlation between bulk modulus and the loss of crystallinity is complex, see SI FigureS14, with the absence of any obvious correlation. The finding is fascinating, and is ressembling the currently poor understanding of the thermodynamic and kinetic procceses of how defects are incorporated into the MOF framework. In turn our results pave the way for experimentally guided computational studies, and emphasize the complex landscape of parameters scientists face when trying to understand and establish structure-property relationships in defective MOFs. Our work presents the first attempt to experimentally establish structure-property relations in defective MOFs, opening new avenues for future synthetic work in this area.

ASSOCIATED CONTENT

Supporting Information

The Supporting Information is available free of charge on the ACS Publications website. Information related to synthesis, additional experimental and analytical details from page S1 to S18 (PDF) are available in the SI.

AUTHOR INFORMATION

Corresponding Author

*Gregor.Kieslich@tum.de
*Roland.Fischer@tum.de

Present Addresses

Chair of Inorganic and Metal-Organic Chemistry, Catalysis Research Center, Department of Chemistry, Technical University of Munich, Ernst-Otto-Fischer-Straße 1, 85748 Garching, Germany.

Notes
The authors declare no competing financial interests.

ACKNOWLEDGMENT

REFERENCES

(1) Tilley, R. J. D., *Defects in Solids*. John Wiley and Sons: Weinheim, Germany, 2008.
(2) Busch, G., *Eur. Phys. J.* 1989, 10 (4), 254.
(3) Tallon, J. L.; Bernhard, C.; Shaked, H.; Hitterman, R. L.; Jorgensen, J. D., *Phys. Rev. B* 1995, 51 (18), 12911-12914.
(4) Yaghi, O. M.; O'Keeffe, M.; Ockwig, N. W.; Chae, H. K.; Eddaoudi, M.; Kim, J., *Nature* 2003, 423, 705-714.
(5) Rimoldi, M.; Howarth, A. J.; DeStefano, M. R.; Lin, L.; Goswami, S.; Li, P.; Hupp, J. T.; Farha, O. K., *ACS Catal.* 2017, 7 (2), 997-1014.
(6) Kozachuk, O.; Luz, I.; Llabrés i Xamena, F. X.; Noei, H.; Kauer, M.; Albada, H. B.; Bloch, E. D.; Marler, B.; Wang, Y.; Muhler, M.; Fischer, R. A., *Angew. Chem. Int. Ed.* 2014, 53 (27), 7058-7062.
(7) Cirujano, F. G.; Corma, A.; Llabrés i Xamena, F. X., *Chem. Eng. Sci.* 2015, 124, 52-60.
(8) Kreno, L. E.; Leong, K.; Farha, O. K.; Allendorf, M.; Van Duyne, R. P.; Hupp, J. T., *Chem. Rev.* 2012, 112 (2), 1105-1125.
(9) Zhang, Y.; Yuan, S.; Feng, X.; Li, H.; Zhou, J.; Wang, B., *J. Am. Chem. Soc.* 2016, 138 (18), 5785-5788.
(10) Li, J.-R.; Sculley, J.; Zhou, H.-C., *Chem. Rev.* 2012, 112 (2), 869-932.
(11) Zhang, H.; Hou, J.; Hu, Y.; Wang, P.; Ou, R.; Jiang, L.; Liu, J. Z.; Freeman, B. D.; Hill, A. J.; Wang, H., *Sci. Adv.* 2018, 4 (2).
(12) Kim, H.; Yang, S.; Rao, S. R.; Narayanan, S.; Kapustin, E. A.; Furukawa, H.; Umans, A. S.; Yaghi, O. M.; Wang, E. N., *Science* 2017, 356 (6336), 430-434.
(13) Rieth, A. J.; Yang, S.; Wang, E. N.; Dincă, M., *ACS Cent. Sci.* 2017, 3 (6), 668-672.
(14) Dissegna, S.; Epp, K.; Heinz, W. R.; Kieslich, G.; Fischer, R. A., *Adv. Mater.* 2018, 0 (0), 1704501.
(15) Fang, Z.; Dürholt, J. P.; Kauer, M.; Zhang, W.; Lochenie, C.; Jee, B.; Albada, B.; Metzler-Nolte, N.; Pöppl, A.; Weber, B.; Muhler, M.; Wang, Y.; Schmid, R.; Fischer, R. A., *J. Am. Chem. Soc.* 2014, 136 (27), 9627-9636.
(16) Cliffe, M. J.; Hill, J. A.; Murray, C. A.; Coudert, F.-X.; Goodwin, A. L., *Phys. Chem. Chem. Phys.* 2015, 17 (17), 11586-11592.
(17) Bennett, T. D.; Cheetham, A. K., *Acc. Chem. Res.* 2014, 47 (5), 1555-1562.
(18) Bennett, T. D.; Yue, Y.; Li, P.; Qiao, A.; Tao, H.; Greaves, N. G.; Richards, T.; Lampronti, G. I.; Redfern, S. A. T.; Blanc, F.; Farha, O. K.; Hupp, J. T.; Cheetham, A. K.; Keen, D. A., *J. Am. Chem. Soc.* 2016, 138 (10), 3484-3492.
(19) Valenzano, L.; Civalleri, B.; Chavan, S.; Bordiga, S.; Nilsen, M. H.; Jakobsen, S.; Lillerud, K. P.; Lamberti, C., *Chem. Mater.* 2011, 23 (7), 1700-1718.
(20) Cavka, J. H.; Jakobsen, S.; Olsbye, U.; Guillou, N.; Lamberti, C.; Bordiga, S.; Lillerud, K. P., *J. Am. Chem. Soc.* 2008, 130 (42), 13850-13851.
(21) Shearer, G. C.; Chavan, S.; Bordiga, S.; Svelle, S.; Olsbye, U.; Lillerud, K. P., *Chem. Mater.* 2016, 28 (11), 3749-3761.
(22) Vermoortele, F.; Bueken, B.; Le Bars, G.; Van de Voorde, B.; Vandichel, M.; Houthoofd, K.; Vimont, A.; Daturi, M.; Waroquier, M.; Van Speybroeck, V.; Kirschhock, C.; De Vos, D. E., *J. Am. Chem. Soc.* 2013, 135 (31), 11465-11468.
(23) Ravon, U.; Savonnet, M.; Aguado, S.; Domine, M. E.; Janneau, E.; Farrusseng, D., *Microporous Mesoporous Mater.* 2010, 129 (3), 319-329.
(24) Cliffe, M. J.; Wan, W.; Zou, X.; Chater, P. A.; Kleppe, A. K.; Tucker, M. G.; Wilhelm, H.; Funnell, N. P.; Coudert, F.-X.; Goodwin, A. L., *Nat. Commun.* 2014, 5, 4176.
(25) Tan, J. C.; Cheetham, A. K., *Chem. Soc. Rev.* 2011, 40 (2), 1059-1080.
(26) McKellar, S. C.; Moggach, S. A., *Acta Crystallogr. B* 2015, 71 (6), 587-607.
(27) Yot, P. G.; Vanduyfhuys, L.; Alvarez, E.; Rodriguez, J.; Itie, J.-P.; Fabry, P.; Guillou, N.; Devic, T.; Beurroies, I.; Llewellyn, P. L.; Van Speybroeck, V.; Serre, C.; Maurin, G., *Chem. Sci.* 2016, 7 (1), 446-450.
(28) Henke, S.; Wharmby, M. T.; Kieslich, G.; Hante, I.; Schneemann, A.; Wu, Y.; Daisenberger, D.; Cheetham, A. K., *Chem. Sci.* 2018, 9 (6), 1654-1660.
(29) Ferey, G.; Serre, C., *Chem. Soc. Rev.* 2009, 38 (5), 1380-1399.
(30) Hu, Y. H.; Zhang, L., *Phys. Rev. B* 2010, 81 (17), 174103.
(31) Chapman, K. W.; Halder, G. J.; Chupas, P. J., *J. Am. Chem. Soc.* 2009, 131 (48), 17546-17547.
(32) Gascon, J.; Corma, A.; Kapteijn, F.; Llabrés i Xamena, F. X., *ACS Catal.* 2014, 4 (2), 361-378.
(33) Rogge, S. M. J.; Wieme, J.; Vanduyfhuys, L.; Vandenbrande, S.; Maurin, G.; Verstraelen, T.; Waroquier, M.; Van Speybroeck, V., *Chem. Mater.* 2016, 28 (16), 5721-5732.
(34) Coudert, F.-X.; Fuchs, A. H., *Coord. Chem. Rev.* 2016, 307, Part 2, 211-236.
(35) Thornton, A. W.; Babarao, R.; Jain, A.; Trousselet, F.; Coudert, F. X., *Dalton Trans.* 2016, 45 (10), 4352-4359.
(36) Dürholt, J. P.; Julian, K.; Rochus, S., *Eur. J. Inorg. Chem.* 2016, 2016 (27), 4517-4523.
(37) Sarkisov, L., *Dalton Trans.* 2016, 45 (10), 4203-4212.
(38) Semino, R.; Ramsahye, N. A.; Ghoufi, A.; Maurin, G., *Microporous Mesoporous Mater.* 2017, 254, 184-191.
(39) Brooks, N. J.; Gauthe, B. L.; Terrill, N. J.; Rogers, S. E.; Templer, R. H.; Ces, O.; Seddon, J. M., *Rev. Sci. Instrum.* 2010, 81 (6), 064103.
(40) Hobday, C. L.; Marshall, R. J.; Murphie, C. F.; Sotelo, J.; Richards, T.; Allan, D. R.; Düren, T.; Coudert, F. X.; Forgan, R. S.; Morrison, C. A.; Moggach, S. A.; Bennett, T. D., *Angew. Chem. Int. Ed.* 2016, 55 (7), 2401-2405.
(41) Yot, P. G.; Yang, K.; Ragon, F.; Dmitriev, V.; Devic, T.; Horcajada, P.; Serre, C.; Maurin, G., *Dalton Trans.* 2016, 45 (10), 4283-4288.
(42) Chapman, K. W.; Halder, G. J.; Chupas, P. J., *J. Am. Chem. Soc.* 2008, 130 (32), 10524-10526.
(43) Yang, K.; Zhou, G.; Xu, Q., *RSC Adv.* 2016, 6 (44), 37506-37514.
(44) Jaffe, A.; Lin, Y.; Beavers, C. M.; Voss, J.; Mao, W. L.; Karunadasa, H. I., *ACS Cent. Sci.* 2016, 2 (4), 201-209.
(45) Kieslich, G.; Forse, A. C.; Sun, S.; Butler, K. T.; Kumagai, S.; Wu, Y.; Warren, M. R.; Walsh, A.; Grey, C. P.; Cheetham, A. K., *Chem. Mater.* 2016, 28 (1), 312-317.
(46) Birch, F., *Phys. Rev.* 1947, 71 (11), 809-824.

Authors are required to submit a graphic entry for the Table of Contents (TOC) that, in conjunction with the manuscript title, should give the reader a representative idea of one of the following: A key structure, reaction, equation, concept, or theorem, etc., that is discussed in the manuscript. Consult the journal's Instructions for Authors for TOC graphic specifications.

Insert Table of Contents artwork here